

Delayed-Photoneutron Calculator for 37-Element Fuel Bundle in CANDU-6 Lattice

Yanuar Ady Setiawan^{a,b}, Douglas A. Fynan^{a*}

^aDepartment of Nuclear Engineering, Ulsan National Institute of Science and Technology (UNIST), 50 UNIST-gil, Eonyang-eup, Ulsu-gun, Ulsan, 22919, Republic of Korea

^bDepartment of Nuclear Engineering and Engineering Physics, Faculty of Engineering, Universitas Gadjah Mada (UGM), Yogyakarta, 55281, Indonesia

*Corresponding author: dfynan@unist.ac.kr

1. Introduction

Hard gamma rays emitted during fission-product decay can produce photoneutrons in heavy water reactors (HWR) and beryllium reflectors due to the low neutron separation energies of ⁹Be and D. Some delayed-photoneutron precursors have much longer half-lives than the conventional 6-group delayed-neutron precursors, so additional delayed-photoneutron groups should be considered in HWR analysis.

Delayed-photoneutron group data are plant/design specific and dependent on the particular fuel design and fuel cycle used in that particular HWR, whereas conventional delayed neutrons are only dependent on the precursor yields of the fissioning isotopes and branching ratios for neutron decay. Delayed-photoneutron group data have been mainly derived from a patch work of legacy experiments, mainly neutron irradiations of fissile isotopes [1], fissioning assemblies [2], and integral zero-power reactor measurements [3], and until recently, no detailed isotopic analysis of precursors have been performed [4]. Secondly, delayed-photoneutron production in HWR involves the radiation transport of gamma rays (produced in the fuel) through the fuel bundle and coolant channel and into the D₂O moderator. Thus, delayed photoneutrons are related to both intrinsic properties of the precursor and daughter isotope fission yields and decay scheme (characteristic gamma-ray energies and intensities) and the macroscopic properties of the operating HWR which influence the photon attenuation including reactor materials, lattice geometry, and space-time power distribution and burnup determining the spatial distribution of the gamma-ray source. The only detailed photon transport analysis available in the literature appears to be for FUGEN (ATR/Advanced Test Reactor), a light-water boiling, vertical-pressure tube HWR reactor operated in Japan [5].

This paper presents a delayed-photoneutron yield calculator for the CANDU-6 lattice and 37-element fuel bundle. A response function giving photoneutron yield probability as a function of photon energy and source position (Rings 1-4 in fuel bundle) was developed through numerous Monte-Carlo (MC) radiation transport simulations of monoenergetic photons in the CANDU-6 lattice. When provided with element-wise burnup history and fission product decay scheme data (discrete gamma-ray energy and intensity), the calculator gives the delayed-photoneutron yields for any 37-element fuel bundle in a CANDU-6 reactor.

2. Delayed-Photoneutron Calculator

2.1 CANDU Lattice and 37-Element Fuel Bundle Model

A unit cell model of the CANDU-6 lattice and standard 37-element fuel bundle was developed for fixed-source photon transport calculations with the UNIST Monte Carlo Code MCS [6]. The fuel channel comprised of concentric calandria tube, insulating gas annulus, pressure tube, and coolant is surrounded by the D₂O moderator box (28.575 cm × 28.575 cm × 49.82 cm). The mean free path (mfp) of fission-product gamma rays in heavy water is between 20 cm and 35 cm [7], so reflecting boundary conditions are applied to the moderator box surface to simulate photon streaming from adjacent fuel channels noting that HWRs with tighter channel pitch will generally have lower photoneutron yields due to increased parasitic attenuation in the fuel channels. Fuel channel dimensions are given in Fig. 1, while Table I summarizes the material compositions. Coolant and moderator D-enrichments in atom% are 97.5% and 99.8%, respectively. In ascending order, the central fuel pin is designated as Ring-1 to the outer fuel pins as Ring-4.

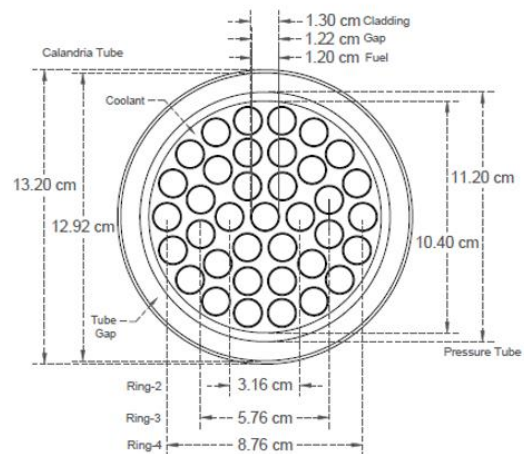


Fig. 1. CANDU 37-element fuel bundle cross section.

Table I: CANDU-6 Lattice Materials and Properties

Material	Region	ρ (g/cm ³)	T (°C)
UO ₂	Fuel Pin	10.420	690
Zircaloy-4	Cladding	6.550	627
Zircaloy-2	Pressure Tube	6.550	227
	Calandria Tube		127
D ₂ O	Coolant	0.813	290 (10 MPa)
D ₂ O	Moderator	1.085	70 (1 atm)

2.2 Photon Fixed-Source Definition and Flux Tallies

Thousands of isotopes and isomers can be generated as fission products. The fission-product concentrations are fuel-ring dependent according to local power distribution and burnup affecting proportions of ^{235}U and ^{239}Pu fission. Any radioactive fission product with a Q-value greater than 2.2259 MeV has the energetic potential to produce at least one gamma ray capable of inducing the $\text{D}(\gamma, \text{n})^1\text{H}$ reaction. Direct simulation of each isotope-specific discrete gamma-ray spectrum scaled to the region-wise concentrations is not practical because most of the decay schemes of the dozens of delayed-photoneutron precursors have multiple gamma lines above the threshold energy and each one of 4,560 fuel bundles in a CANDU-6 has a unique burnup. Monoenergetic photon fixed sources were prepared on a fine energy grid from the threshold to 8 MeV to bound the gamma-ray energies of fission products. A forward MCS simulation was performed at each source energy E_s to give the multi-group photon flux $\phi_{r,j}$ in region volumes V_r of the unit cell model from which the photoneutron yield Y_r in each region can be calculated by

$$Y_r(E_s, r_s) = V_r \sum_i N_{r,i} \sum_j v_i(\bar{E}_j) \sigma_i(\bar{E}_j) \phi_{r,j} \quad (1)$$

The number density of the isotope in V_r interacting with the photon through photoneuclear reaction channel i (photoneutron reaction or photofission) is designated $N_{r,i}$. The neutron yield v_i and microscopic cross section σ_i of reaction channel i are calculated at the midpoint energy \bar{E}_j of energy group j . An adaptive energy group structure was adopted to minimize discretization error of Eq. (1) [7]. Multi-group photon-flux tabulation and reaction-rate calculation explicitly accounts for photoneutron production after Compton scattering of the source-photon which is negligible for gamma-ray energies near the threshold energy but is over 20% of total yield for 5 MeV source-photon.

Photon attenuation is a dependent on source position within the fuel bundle, so the MCS simulations were repeated by uniformly distributing the isotropic photon source within one of five source regions r_s : fuel Rings 1-4 and moderator region. Hard-gamma-emitting activation products such as ^{16}N can be generated in the moderator. The photoneutron calculator stores Eq. (1) evaluations for all E_s and r_s and linearly interpolates to give photoneutron yield for any discrete gamma-ray energy and source location.

Figure 2 shows the D and ^{238}U photoneuclear reaction cross sections from ENDF/B-VII.1 library. Deuterium cross section is always small (mb) but the low threshold energy enables photoneutron production from gamma rays; the vast majority of delayed-photoneutrons will be produced from $\text{D}(\gamma, \text{n})^1\text{H}$. A few short-lived radionuclides with large Q-value have hard gamma lines where photofission and (γ, n) reaction could occur in the fuel heavy isotopes, so the calculator tabulates the photoneuclear reaction rates involving ^{238}U and ^{235}U .

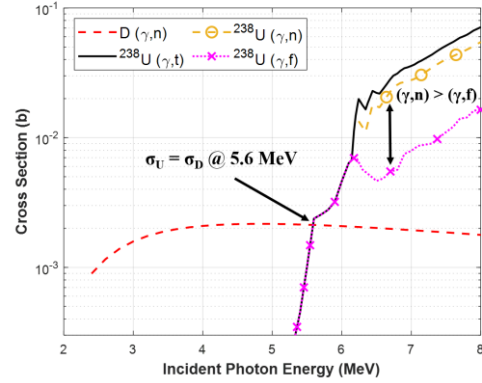


Fig. 2. Photonuclear cross sections for deuterium and ^{238}U .

3. Results for CANDU-6 Lattice

3.1 Photon attenuation effect of source location

The total photoneutron yield response function curves are shown in Fig. 3. Each source-region curve is the summation of photoneutrons produced in the moderator, coolant, and fuel from photons originating from the source region. The infinite- D_2O curve is the upper bound case (point photon source in an infinite heavy water medium). The relative differences between curves reflects the source-location dependency of photon attenuation. Ring-1 (center pin) source has the lowest photoneutron yields because the gamma rays must stream through the other three fuel rings, pressure tube, and calandria tube before producing a photoneutron in the moderator. Ring-4 source has photoneutron yields 60%-70% greater than Ring-1 source because over 50% of gamma rays have initial emission angle subtended by the moderator volume. A single fission event in Ring-4 has a higher importance to delayed-photoneutron fraction than a single fission event in any of the other fuel rings. Furthermore, the 37-element power distribution is significantly peaked in Ring-4 as neutrons diffuse back into the fuel channel after thermalizing in the moderator. Ring-4 fuel elements achieve higher burnup and higher proportion of plutonium fission, so changes in delayed-photoneutron precursor concentrations due to fission yield are more pronounced.

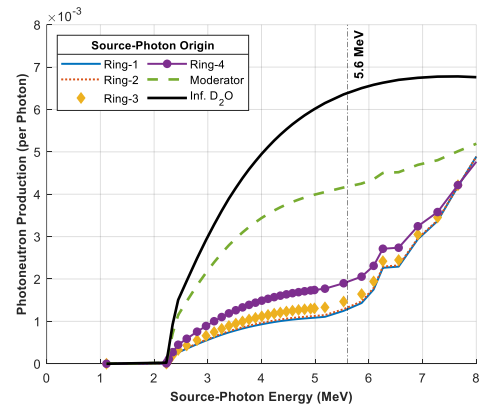


Fig. 3. Total photoneutron yield in lattice as function of source-photon energy and location.

The strong energy dependence of the relative difference between the infinite-D₂O source and moderator source demonstrates the shielding effect of the fuel channels and photon streaming through the moderator. The higher-energy gamma rays have longer mean-free-paths. Plant-to-plant variation in fuel lattice geometry and pitch will affect the delayed-photoneutron fraction. In particular, some heavy water research reactors where integral delayed-photoneutron measurements have been performed have entirely different fuel design and lattice than large power HWRs such as the CANDU-6.

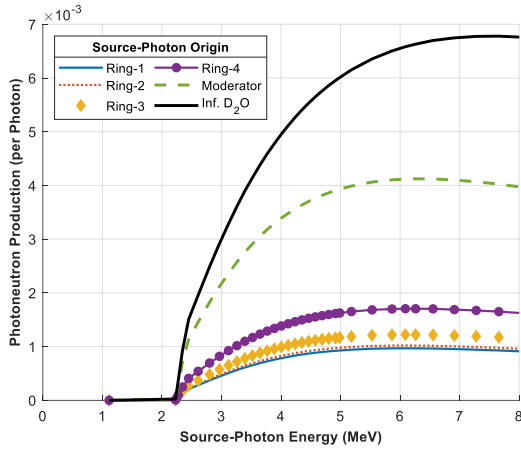


Fig. 4. Photoneutron yield in moderator as function of source-photon energy and location.

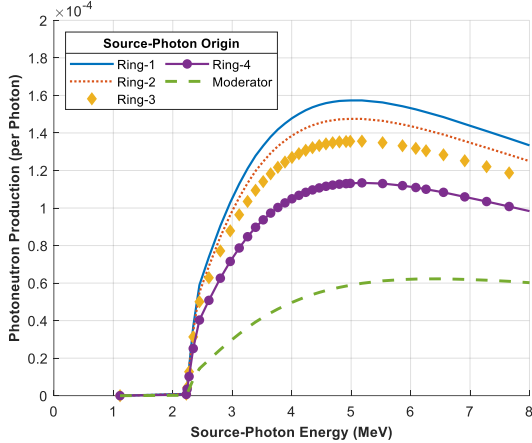


Fig. 5. Photoneutron yield in coolant as function of source-photon energy and location.

Figures 4, 5, and 6 show the individual region contributions to total photoneutron yield from production in moderator, coolant, and fuel, respectively. Below 5 MeV, approximately 90% of all photoneutrons are generated in the moderator and the remainder in the coolant. In the CANDU-6 lattice, the moderator volume contains an order of magnitude more D₂O than the coolant channel. The source-location trend is reversed for photoneutron production in the coolant with Ring-1 source having the highest (absolute) coolant yield. The coolant yield for Ring-1 source also has a higher relative yield of approximately 14% of the Ring-1 total photoneutron yield. Above 5.6 MeV, photonuclear

reactions in the fuel become important and the yields are the same order of magnitude as photoneutron production in the heavy water regions. Ring-1 source has highest fuel yields because all Ring-1 photons stream through multiple fuel pins.

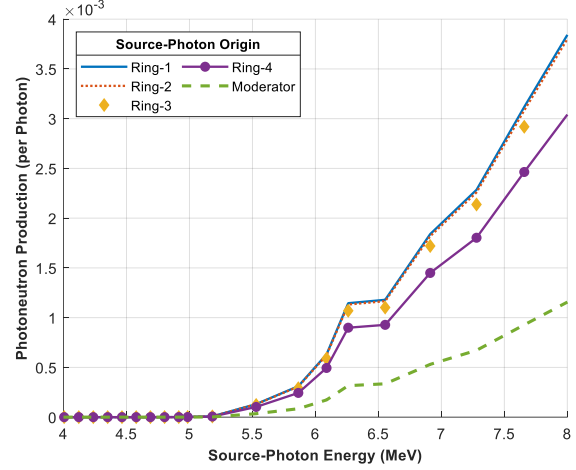


Fig. 6. Photoneutron yield in fuel as function of source-photon energy and location.

Table II: Photoneutron Yield per Precursor Decay

Fission Product	Source-Photon Origin (r_s)			
	Ring-1	Ring-2	Ring-3	Ring-4
^{97m} Y	6.83E-6	7.08E-6	8.26E-6	1.12E-5
⁹⁷ Y	2.84E-4	2.94E-4	3.42E-4	4.57E-4
⁹³ Rb	2.39E-4	2.47E-4	2.87E-4	3.85E-4
⁹¹ Kr	1.04E-4	1.07E-4	1.25E-4	1.70E-4
⁸⁸ Br	4.17E-4	4.32E-4	4.99E-4	6.60E-4
⁹⁵ Sr	1.36E-4	1.41E-4	1.64E-4	2.21E-4
¹³⁷ I	7.73E-5	8.02E-5	9.32E-5	1.25E-4
¹⁴⁵ La	1.04E-5	1.08E-5	1.28E-5	1.76E-5
^{136m} I	2.31E-6	2.39E-6	2.79E-6	3.76E-6
⁸⁷ Br	4.20E-4	4.36E-4	5.06E-4	6.75E-4
⁹¹ Rb	3.36E-4	3.49E-4	4.05E-4	5.42E-4
¹⁴⁰ Cs	8.91E-5	9.23E-5	1.08E-4	1.46E-4
¹³⁶ I	1.18E-4	1.22E-4	1.41E-4	1.90E-4
⁹⁰ Rb	3.33E-4	3.45E-4	4.00E-4	5.33E-4
⁸⁹ Kr	1.15E-4	1.19E-4	1.38E-4	1.85E-4
^{90m} Rb	3.00E-4	3.11E-4	3.62E-4	4.85E-4
⁹⁵ Y	8.96E-5	9.29E-5	1.08E-4	1.45E-4
⁸⁹ Rb	5.70E-5	5.91E-5	6.92E-5	9.40E-5
⁸⁸ Rb	1.59E-5	1.65E-5	1.92E-5	2.60E-5
⁸³ Se	1.42E-5	1.47E-5	1.74E-5	2.41E-5
¹³⁸ Cs	3.52E-5	3.64E-5	4.27E-5	5.80E-5
⁸⁷ Kr	4.94E-5	5.11E-5	6.01E-5	8.19E-5
¹⁴² La	1.63E-4	1.69E-4	1.98E-4	2.68E-4
⁸⁸ Kr	7.70E-5	7.97E-5	9.42E-5	1.30E-4
¹⁴⁰ La	1.29E-5	1.34E-5	1.57E-5	2.16E-5

3.2 Photoneutron yields of fission products

Table II summarizes photoneutron yields for a partial list of precursors identified in [4] and with additional contributions from our cursory survey of fission product decay schemes. Isotope decay schemes were obtained from ENDF/B-VII.1 radioactive decay data (ENDF/B-VIII.0 for ¹⁴⁵La). Discrete gamma-ray energies were

evaluated in the calculator, and the photoneutron yields for each source region were scaled by the absolute intensities of the gamma lines to give yield per decay of precursor.

Table III illustrates the importance of gamma-ray energy by comparing yields per gamma line for ^{88}Kr to ^{97}Y . Despite having similar total intensities of gammas above the threshold energy, ^{97}Y yield is almost a factor of four greater than ^{88}Kr because the D photoneutron cross section is small at 2.392 MeV, the dominant ^{88}Kr line. In the actual fuel, saturation activity is proportional to the cumulative fission yield χ_c of the precursor which is a function of the fissioning isotope.

Table III: Decay-Scheme Dependence of Photoneutron Yields from ^{88}Kr and ^{97}Y

^{88}Kr (39.7%- γ)		^{235}U $\chi_c = 3.5\%$		^{239}Pu $\chi_c = 1.2\%$	
		Source-Photon Origin			
E_γ (MeV)	Abs. Intensity	Ring-1	Ring-2	Ring-3	Ring-4
2.232	3.39%	3.0E-7	3.2E-7	3.7E-7	5.2E-7
2.260	0.03%	1.4E-8	1.4E-8	1.7E-8	2.4E-8
2.352	0.73%	1.2E-6	1.3E-6	1.5E-6	2.1E-6
2.365	0.03%	5.6E-8	5.8E-8	6.9E-8	9.6E-8
2.392	34.60%	7.2E-5	7.5E-5	8.9E-5	1.2E-4
2.409	0.10%	2.3E-7	2.4E-7	2.9E-7	4.0E-7
2.536	0.04%	1.3E-7	1.4E-7	1.6E-7	2.2E-7
2.548	0.62%	2.0E-6	2.1E-6	2.4E-6	3.3E-6
2.771	0.15%	6.6E-7	6.9E-7	8.0E-7	1.1E-6
Total Yield		7.7E-5	8.0E-5	9.4E-5	1.3E-4
^{97}Y (41.9%- γ)		^{235}U $\chi_c = 2.6\%$		^{239}Pu $\chi_c = 1.3\%$	
		Source-Photon Origin			
E_γ (MeV)	Abs. Intensity	Ring-1	Ring-2	Ring-3	Ring-4
2.743	6.52%	2.8E-5	2.9E-5	3.4E-5	4.6E-5
3.288	18.10%	1.3E-4	1.3E-4	1.5E-4	2.0E-4
3.401	14.12%	1.0E-4	1.1E-4	1.3E-4	1.7E-4
3.550	3.11%	2.5E-5	2.6E-5	3.0E-5	4.0E-5
Total Yield		2.8E-4	2.9E-4	3.4E-4	4.6E-4

3.3 Photoneutron yield from activation product ^{16}N

In a nuclear reactor, isotopes undergoing neutron decay can only be generated through fission, but many neutron activation reactions on stable fission products and reactor materials produce delayed-photoneutron precursors [8]. High Q-value ^{16}N (7.13 s $T_{1/2}$) is produced from the ^{16}O (n,p) reaction in the UO_2 fuel and D_2O (coolant and moderator). Table IV provides the gamma-line photoneutron yields for ^{16}N . Per decay, ^{16}N produces a factor of 10 greater yield than most fission product due to the high intensity and high energy gammas. Interestingly, 27-43% of global photoneutrons produced by ^{16}N within the fuel are from ^{238}U photonuclear reactions. Also, gammas produced in the moderator can stream into the fuel channel producing photoneutrons. Although a ^{16}N decay in the coolant channel will produce photoneutrons, most of the ^{16}N precursors are transported and decay throughout the reactor coolant system and do not contribute to the delayed-neutron fraction.

Table IV: Photoneutron Yields from ^{16}N Decay

E_γ (MeV)	Int. (%)	Source-Photon Origin				
		R-1	R-2	R-3	R-4	M
2.74	0.82	3.5E-6	3.6E-6	4.3E-6	5.8E-6	1.4E-5
2.82	0.13	6.1E-7	6.4E-7	7.4E-7	1.0E-6	2.5E-6
6.13	67.0	1.3E-3 (40%)*	1.3E-3 (39%)	1.4E-3 (34%)	1.6E-3 (24%)	2.9E-3 (4.7%)
6.92	0.04	1.1E-6	1.1E-6	1.2E-6	1.2E-6	1.8E-6
7.12	4.90	1.6E-4 (66%)	1.6E-4 (65%)	1.6E-4 (60%)	1.7E-4 (48%)	2.3E-4 (13%)
8.87	0.08	6.0E-6	6.0E-6	5.8E-6	5.4E-6	4.6E-6
Total Yield		1.4E-3 (43%)	1.4E-3 (42%)	1.5E-3 (37%)	1.8E-3 (27%)	3.2E-3 (5.3%)

*relative contribution from ^{238}U photonuclear reactions in fuel

ACKNOWLEDGEMENTS

This research was supported by the National Research Foundation of Korea (NRF) grant funded by the Korean government (MSIT) (No. 2019M2D2A1A01034124) and Ulsan National Institute of Science & Technology Internal Project (No. 1.180088.01).

REFERENCES

- [1] S. Bernstein, W. M. Preston, G. Wolfe, R.E. Slattery, Yields of Photo-Neutrons from U^{235} Fission Products in Heavy Water, Physical Review, Vol.71(9), p.573-582, 1947.
- [2] N. P. Baumann, R. L. Currie, D. J. Pellarin, "Production of Delayed Photoneutrons from ^{235}U in Heavy Water Moderator, Savannah River Laboratory", DP-MS-73-39 CONF-731101-40 - Du Pont de Nemours (E.I.) and Co., Savannah River Lab., Aiken, South Carolina 1973.
- [3] W. W. Graham III, D. S. Harmer, C. E. Cohn, Accurate Delayed-Neutron Parameter Measurements in a Heavy-Water Reactor, Nuclear Science and Engineering, Vol.38(1), p.33-41, 1969.
- [4] E. T. Rand, J. E. Atfield, L. R. Yaraskavitch, Microscopic Calculation of Delayed-Photoneutron Production in D_2O using GEANT4, Annals of Nuclear Energy, Vol.129, p.390-398, 2019.
- [5] Y. Kaneko, Effect of Phot-Reactions on the Effective Yield of Delayed Neutrons in the Pressure Tube Type Heavy Water Reactor, Journal of Nuclear Science and Technology, Vol.8(1), p.34-40, 1971.
- [6] M. Lemaire, H. Lee, B. Ebiwonjumi, C. Kong, W. Kim, Y. Jo, J. Park, D. Lee, Verification of Photon Transport Capability of UNIST Monte Carlo Code MCS, Computer Physics Communication, Vol.231, p.1-18, 2018.
- [7] D. A. Fynan, Y. Seo, G. Kim, S. Barros, M. J. Kim, Photoneutron Production in Heavy Water Reactor Fuel Lattice from Accelerator-Driven Bremsstrahlung, Annals of Nuclear Energy, Vol.155, p.1-13, 2021.
- [8] Y. A. Setiawan, D. A. Fynan, Neutron Capture on Stable Fission Product ^{139}La Contribution to Delayed-Photoneutrons in Heavy Water Reactors, Transactions of the American Nuclear Society, Vol.123, p.1285-1286, 2020.